Comparative Study of Various Approaches For Joint Demosaicing And Subpixel Based Downsampling In Bayer Images

Lekshmi P R

***Abstract*— A portable device such as a digital camera with a single sensor and Bayer color filter array (CFA) requires demosaicing to reconstruct a full color image. To display a high resolution image on a low resolution LCD screen of the portable device, it must be down-sampled. The two steps, demosaicing and down-sampling, influence each other. On one hand, the color artifacts introduced in demosaicing may be magnified when followed by down-sampling; on the other hand, the detail removed in the down-sampling cannot be recovered in the demosaicing. Therefore, it is very important to consider simultaneous demosaicing and down-sampling. In this paper, a fast frequency domain analysis approach and an adaptive approach for joint demosaicing and subpixel-based down-sampling of single sensor Bayer images is described. In frequency domain approach for joint demosaicing and subpixel-based down-sampling (FFAJDSD), we integrate demosaicing into down-sampling by directly performing subpixel based down-sampling in the Bayer domain.In Adaptive Joint Demosaicing and Subpixel based Down-sampling scheme (AJDSD),subpixel-based down-sampling is adaptively and directly applied in Bayer domain, without the process of demosaicing.When compared with conventional methods, these two approaches achieve superior performance improvements.**

Index Terms— **Demosaicing, down-sampling, subpixel rendering.**

I. INTRODUCTION

Color image processing has attracted much interest over the past decades. Digital cameras are probably the most popular still image acquisition devices, whose commercial proliferation has significant impact on the research in this area. Instead of using three CCD or CMOS sensors, a single sensor based on the Bayer color filter array (CFA) structure [1] is cost-effective to capture the colorful visual scenes [2].With the Bayer CFA structure, each pixel of image has only one of the three primary colors (red, green, blue) captured, as shown in Fig. 1(a). This type of image is known as "Bayer image". Since the human visual system is most sensitive to green (G) color, half of the pixels in the Bayer CFA are assigned to G channel and the rest of the pixels are equally shared by red (R) and blue (B)channels [1]. In the reconstruction step, two missing color components of each pixel in the Bayer image are reconstructed by exploiting the correlation among different pixels and color components, and such a reconstruction process is known as demosaicing [2]. Besides demosaicing, another important problem for rendering an image on a low resolution screen of portable devices such as a digital camera and a smart phone is down-sampling. Currently, available portable devices are capable of capturing images with multiple mega-pixel resolution. Also high resolution displays are becoming more and more popular in high-end smart phones and are indeed very attractive to consumers. To achieve higher apparent resolution when displaying high resolution image/video on a relatively low resolution display, subpixel rendering techniques are used. A traditional way to generate a down-sampled full-color image from the Bayer image for rendering is to perform demosaicing followed by down-sampling, as shown in Fig. 2.

However, this approach requires a significant amount of memory, computation, and battery power during the demosaicing stage, e.g., it requires 30 MB to store a 10 mega-pixel full color image. Generally, users would spend a large amount of time on the capture-and-display viewfinder mode or preview mode without actually doing capture-and-store. In such cases, there is no need to store the high resolution Bayer images and the demosaiced images since most of them are discarded finally. Instead, what we need is to generate and display the down-sampled full color image in real-time. Since demosaicing and down-sampling influence each other (i.e., the color artifacts introduced in demosaicing [3] may be magnified in the subsequent down-sampling, and vice versa), to achieve better results, we should consider joint demosaicing and down-sampling in the Bayer domain, as shown in the red block of Fig. 2. Such an idea is inspired by Lukac et al. [4], where they perform color image zooming directly in the Bayer domain. While the capture-and-display camera viewfinder and the preview screen on the portable device typically have resolution much lower than the capture-and- stored image, it is highly desirable to display as much detail as possible on the low-resolution screen of the portable device. Conventional pixel-based down-sampling with an anti-aliasing prefilter causes severe blurring artifacts, as only the low frequency information can be retained in the process. Therefore, we apply the idea of subpixel rendering in down-sampling process to retain more original information.

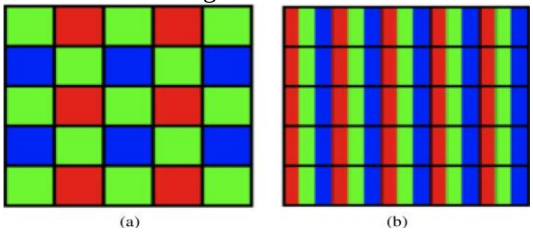

(a) (b)

Manuscript received October 19, 2013.

Lekshmi P R received Btech in Electronics and Communication Engg from CUSAT University Kerala.Currently pursing Mtech in Signal Processing at Govt Engg college, Cherthala under Cochin University Of Science And Technology.

Fig. 1. (a) Bayer CFA of an image sensor with one color per pixel. (b) Subpixel arrangement of pixels in an LCD display.

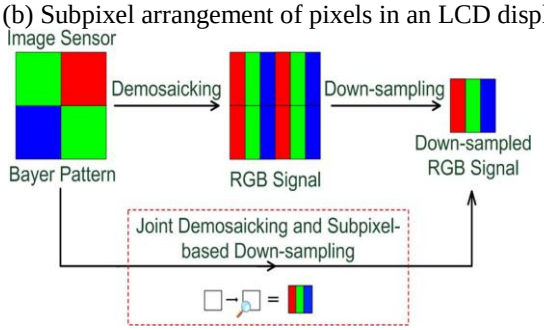

Fig.2. Demosaicing followed by down-sampling scheme and Joint demosaicing and subpixel-based down-sampling scheme.

Subpixel rendering is the technique that can achieve more than one pixel resolution out of one physical LCD pixel. It takes advantage of the fact that each pixel on a color LCD is actually composed of individual red, green and blue subpixel stripes, as shown in Fig. 1(b), to give greater details than simple pixel rendering [5]. Since the number of individual reconstruction points in an LCD can be increased by three times when considering the subpixels, application of subpixel rendering in down-sampling scheme may lead to improvement in apparent resolution. Several subpixel- based down-sampling algorithms for converting a high resolution image to fit a low-resolution LCD display have been proposed recently [7]–[9]. However, all of them require the tri-stimulus values at all the sample points of the large image. One way to apply these approaches is to perform demosaicing to recover high resolution full color image before applying subpixel-based down-sampling. However, as discussed above, such an approach suffers from the problem of high memory usage and high computational complexity. To overcome these problems, in this paper, a fast frequency-domain analysis of joint demosaicing and subpixel-based down-sampling scheme (FFA-JDSD) for single sensor Bayer images is proposed. We will integrate demosaicing into down-sampling by directly performing subpixel- based down-sampling in the Bayer domain, due to which the computational complexity is significantly reduced. Further use frequency domain analysis tool to show that the cut-off frequency of the low-pass filter for JDSD can be effectively extended beyond the Nyquist frequency, resulting in much sharper down-sampled images.

Traditionally, to produce a down-sampled full color image, the CFA image is first recovered to a full color image using conventional demosaicing methods, then the demosaiced full color image is subsampled, as shown in Fig. 3(a). Unfortunately, such approach requires extra storage of full color images, and the color artifacts caused by demosaicing may be magnified in following subsampling. Intuitively, an alternative approach in Fig. 3(b) is down-sampling CFA image followed by conventional demosaicing process. However, it may cause inefficient utilization of the raw sensor data, and the blurring artifacts caused by down-sampling may be magnified during the later demosaicing process. Since demosaicing and downsampling influence each other, it may be advantageous to perform down-sampling and demosaicing jointly and directly in the Bayer domain when possible. Lukac et al. [19] have shown that joint demosaicing and zooming produces good results and is computationally efficient. In, an adaptive joint demosaicing and subpixel-based down-sampling (AJDSD) method Fig. 3(c) is done. By sharing the color information extracted directly from the raw sensor data, a subpixel-based down-sampling scheme is specifically designed.

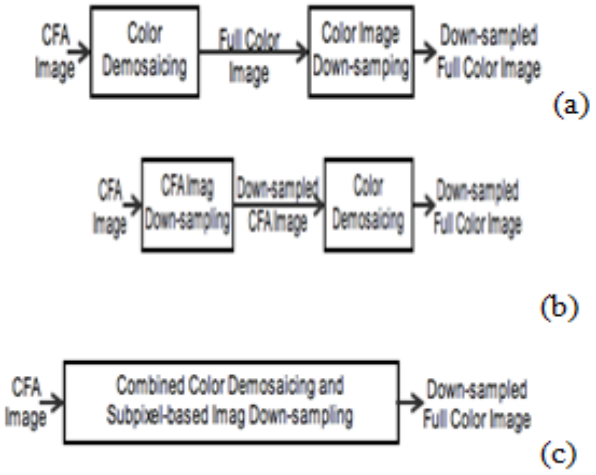

Fig. 3. Image down sampling methods: (a) down sampling demosaicing (b)demosaicing after down sampling (c) proposed joint demosaicing and subpixel based down sampling.

II. COLOR FILTER ARRAY

In photography, CFA or color filter mosaic (CFM), is a mosaic of tiny color filters placed over the pixel sensors of an image sensor to capture color information. The CFA is placed on top of the monochrome image sensor, usually a charge-coupled device (CCD) or complementary metal oxide semiconductor (CMOS) sensor, to acquire the low-resolution color information of the image scene. Color filters are needed because the typical photosensors detect light intensity with little or no wavelength specificity, and therefore cannot separate color information. Since sensors are made of semiconductors they obey solid-state physics.

The color filters filter the light by wavelength range, such that the separate filtered intensities include information about the color of light. For example, the Bayer filter gives information about the intensity of light in red, green, and blue (RGB) wavelength regions. The raw image data captured by the image sensor is then converted to a full-color image (with intensities of all three primary colors represented at each pixel) by a demosaicing algorithm which is tailored for each type of color filter. The spectral transmittance of the CFA elements along with the demosaicing algorithm jointly determines the color rendition. The sensor's pass band quantum efficiency and span of the CFA's spectral responses are typically wider than the visible spectrum, thus all visible colors can be distinguished.

Types of CFAs:

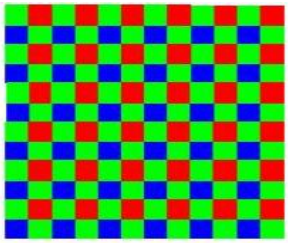

(a)

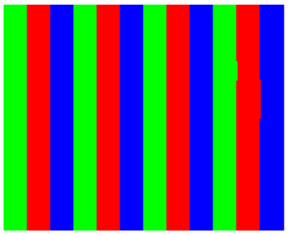

(b)

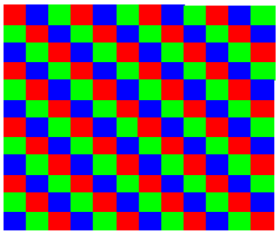

(c)

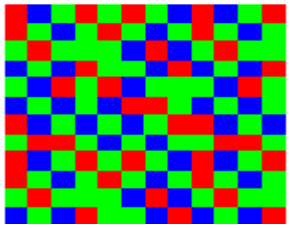

(d)

Fig:4 Types of CFAs (a) Bayer CFA (b) Vertical stripe CFA (C)Diagonal Stripe CFA (d) HVS based CFA

Bayer color filter array is a popular format for digital acquisition of color images. Half of the total numbers of pixels are green (G), while a quarter of the total number is assigned to both red (R) and blue (B). CFA layout should be attributed to the effort of the camera manufacturers to obtain:

i) cost-effective image reconstruction
ii) immunity to color artifacts
iii) robustness of the array to image sensor imperfections
iv) Immunity to optical/electrical cross talk between neighboring pixels.
v) Since the frequency of the G color band is close to the peak of the human luminance frequency response privileging the G color filters in the CFA layout improves the perceived sharpness of the captured image. Manufacturers usually select the CFA layout according to the type and resolution of the image sensor, camera optical system, image processing capabilities of the device, and the intended application. However, once the CFA layout is selected to acquire the CFA image data, the visual quality of the demosaiced full-color image depends on the ability of the demosaicing solution to overcome various spatial, structural and spectral constraints imposed on the single-sensor device during the image formation and color reconstruction. Block diagram representing the traditional two dimensional approach to the multi-frame reconstruction of color images is shown below in fig.5.It is more clear in fig.6.

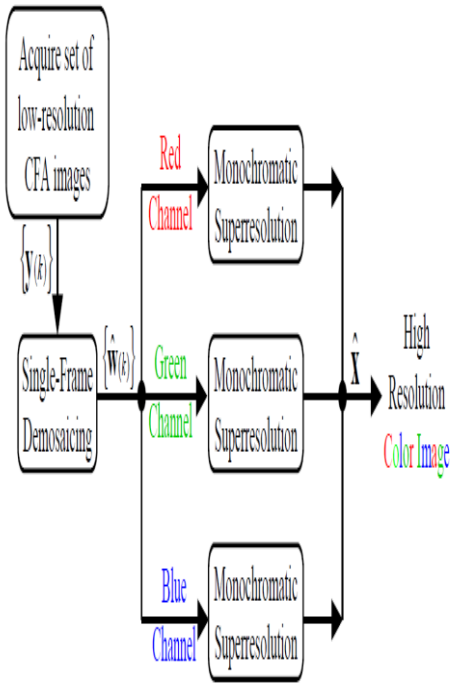

Fig.5. Traditional Two Dimensional Approach to the Multi-Frame Reconstruction of Color Images

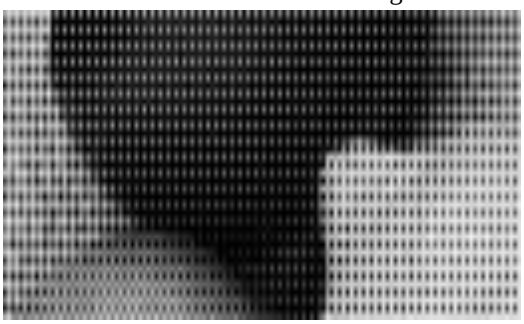

(a)

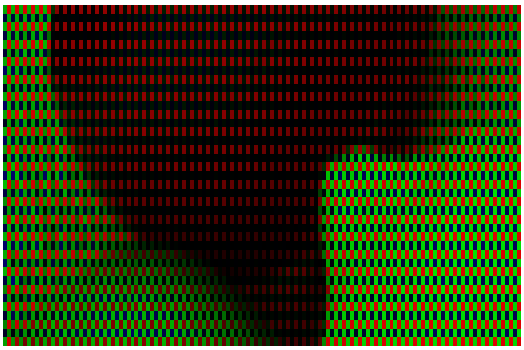

(b)

(c)

Fig.6. Single-sensor imaging: (a) mosaic-like gray-scale CFA image, (b) color variant of the CFA image, (c) demosaiced full-color image.

To display high resolution image on a low resolution screen, it must be downsampled. Color artifacts shown in fig.7 such as zipper effect, blurring, aliasing, false colour may introduce while demosaicing.Images suffer from colour artifacts when samples are not estimated correctly. Most visual artifacts appear at edges and areas of high frequency.

Fig.7. (a) orginal image(b)Bilinearly interpolated from CFA filter samples with colour artifacts

In traditional method,the colour artifacts introduced in demosaicing may be magnified when followed by downsampling.This problem can be solved in FFA-JDSD and AJDSD.

III. DEMOSAICING

When a mosaiced design is used, the captured *raw image* must be processed to produce a full-color image. This processing is called demosaicing and consists of estimating at each pixel the responses of the sensor classes that are not directly available at that pixel.

A. DEMOSAICING ALGORITHMS

A demosaicing algorithm is a digital image processing algorithm used to reconstruct a full color image from the incomplete color samples output from an image sensor overlaid with a color filter array (CFA). Also known as CFA interpolation or color reconstruction. The reconstructed image is typically accurate in uniform-colored areas, but has a loss of resolution (detail and sharpness) and has edge artifacts (for example, the edges of letters have visible color fringes and some roughness).

Algorithms are:

1. Nearest-Neighbour Interpolation:

Simply copies an adjacent pixel of the same color channel (2x2 neighbourhood). It is unsuitable for any application where quality matters.

2. Bilinear Interpolation:

The red value of a non-red pixel is computed as the average of the two or four adjacent red pixels, and similarly for blue and green. Bilinear interpolation generates significant artifacts, especially across edges and other high-frequency content, since it doesn`t take into account the correlation among the RGB values.

3. Cubic Interpolation :

Taking into account more neighbours than in algorithm no. 2 (e.g., 7x7 neighbourhood). Lower weight is given to pixels which are far from the current pixel.

4. Gradient-corrected bilinear interpolation:

An improvement to algorithm no.2.The assumption is that in a luminance/chrominance decomposition, the chrominance components don`t vary much across pixels. It exploits the interchannel correlations between the different color channels and uses the gradients among one color channel, in order to correct the bilinearly interpolated value.

5. Smooth Hue Transition Interpolation:

First, the green values are interpolated using some desired method. By the assumption that hue is smoothly changing across an objects surface, simple equations for the missing colors can be obtained by using the ratios between the known colors and the interpolated green values at each pixel. Problem can occur when the green value is 0, so some simple normalization methods are proposed.

6. Edge weighted Interpolation:

In order to prevent flaws when estimating colors on or around edges. The first step in his procedure is to find the average of the four neighboring green pixels, and classify the neighbors as either high or low in comparison to this average. The green pixel is then defined as an edge if three neighbor pixels share the same classification. If not, then the pixel can either be a part of a corner or a stripe. If two adjacent neighbor pixels have the same classification, then the pixel is a corner. If two opposite pixels have the same classification, then the pixel is a stripe. Using median value, the rest green values are obtained. Later, algorithm5 is used in order to interpolate R and B values. This algorithm better preserves edge details.

IV. SUBPIXEL BASED DOWNSAMPLING

Subpixel-based down-sampling is a method that can potentially improve the apparent resolution of a down-scaled image by controlling individual subpixels rather than pixels. However, the increased luminance resolution often comes at the price of chrominance distortion. A major challenge is to suppress color fringing artifacts while maintaining sharpness.

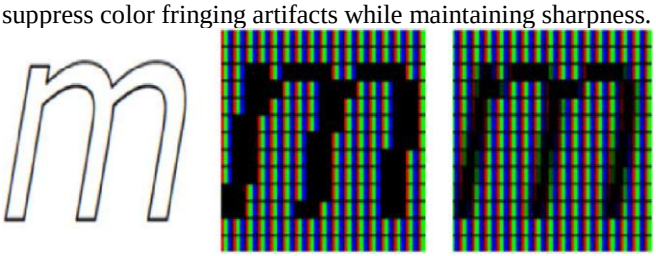

Fig.8. (a) letter "m" in italic (left) (b) whole-pixel rendered "m" with jagged edges (middle)and (c) subpixel rendered "m" with smooth edges (right).

Subpixel rendering, taking advantage of the fact that each pixel on a color LCD is actually composed of individual addressable red, green, and blue subpixel stripes, can increase the apparent resolution of an LCD display while introducing some unpleasant color fringing artifacts Fig. 8 illustrates an example of whole pixel rendering and subpixel rendering by displaying the letter "m" .It is obvious that subpixel rendering can reduce staircase artifacts effectively and reconstruct the shape information more faithfully.A major application of subpixel rendering is image down-sampling for small display.

a)Subpixel Based Downsampling Schemes

Subpixel based downsampling can be done horizontal, diagonal, or anti-diagonal directions. (It does not make sense to sample in vertical direction as RGB subpixels are arranged in horizontal way.)

i) Direct Pixel-based Down-sampling (DPD):

DPD is to perform simple down-sampling by selecting one out of every pixels. (*Direct* means no anti-aliasing filter is applied.) It can incur severe aliasing artifacts in regions with high spatial frequency. This gives an image with irregular spacing,which is bad.

ii) Direct Subpixel-based Down-sampling (DSD):

DSD decimates the red, green, and blue components alternately in the horizontal direction. DSD copies red, green and blue components (i.e., the three subpixels) of the pixel from three different pixels in L. It is clear that DSD considers only the horizontal direction, but not the vertical. DSD can potentially preserve more details than DPD. From fig 9. it is clear that DSD fills in the gaps of the grass, making the grass continuous and sharp at the expense of annoying color artifacts. One of its shortcomings is chrominance distortion.

iii) Diagonal Direct Subpixel-Based Down-Sampling (DDSD):

We observe that the improvement of apparent resolution in DSD tends to happen at regions with vertical edges or edges with vertical component. There is typically no improvement at smooth regions or regions with horizontal edges, due to the fact that in DSD the sampling pattern is merely in a horizontal way, which is parallel to horizontal edges. To achieve improved resolution in both horizontal and vertical directions, DDSD pattern is proposed, changing the sampling direction from horizontal to diagonal as shown in fig 10. DDSD copies the red, green and blue components from three different pixels in the $(i, j)^{th}$ block of L along the diagonal direction. Spectral overlap (aliasing) in DDSD is considerably less than that in DSD, and thus DDSD is more effective in retaining high frequency details than DSD. Therefore, chose to use DDSD instead of DSD.

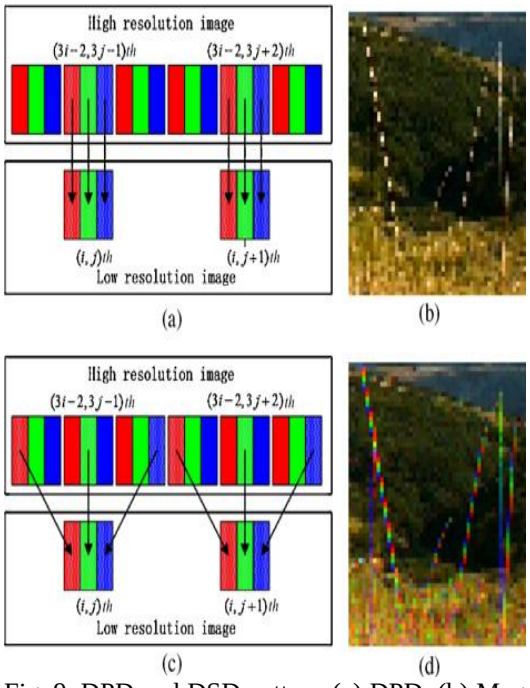

Fig. 9. DPD and DSD patterns(a) DPD. (b) Magnified result of DPD, where "grass" is broken due to aliasing artifacts. (c) DSD. (d) Magnified result of DSD, where "grass" is smooth but has color fringing artifacts.

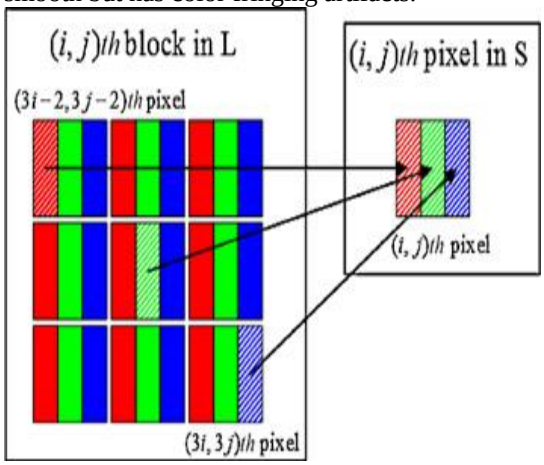

Fig.10.DDSD pattern

Therefore, exploiting subpixels in downsampling brings both opportunity and problem. The opportunity is that we can potentially increase the apparent resolution of a patterned display up to the subpixel resolution. The problem is the associated color distortion.

V. ADAPTIVE APPROACH FOR JOINT DEMOSAICING AND SUBPIXEL-BASED DOWN-SAMPLING

For a mosaic image, each color plane is sampled at a rate less than once per pixel, i.e., 1/3 Bayer samples/subpixel in Fig. 1. Thus at 1: 1 scale, there is not enough input information available for subpixel rendering to take advantage of the increased resolution. Downsampling by a factor of three effectively increases this to the requisite 1 Bayer sample/subpixel for subpixel rendering. A factor of six (in each dimension) is used here since it simplifies the implementation - adjacent 6 × 6 blocks of Bayer data are identical, while 3 × 3 blocks contain alternately more red or blue samples. The approach could be used for any higher down-sampling factor as well. For the simple of presentation,

let us suppose the original Large CFA image (L_{CFA}) is of size 6M × 6N, and the down-sampled Small full color image (S) is of size M × N ×3. the sampling direction adaptively according to the local edge information.Then divided the L_{CFA} into 6×6 blocks so that there are M×N blocks, one for each pixel in the down-sampled low resolution full color images S. Note that in this paper, (i,j) (i = 1,2,……..,M and j = 1,2, …..,N) is used to index the pixel location S. In other words, any (i,j)th pixel of S corresponds to (i, j)th 6×6 block of L_{CFA}, as shown in Fig. 11(a). We further divide one block into nine sub-blocks, which is of size 2 x 2 and indexed by (m, n). (For down-sampling ratio other than six, the size of sub-block can be chosen accordingly.)

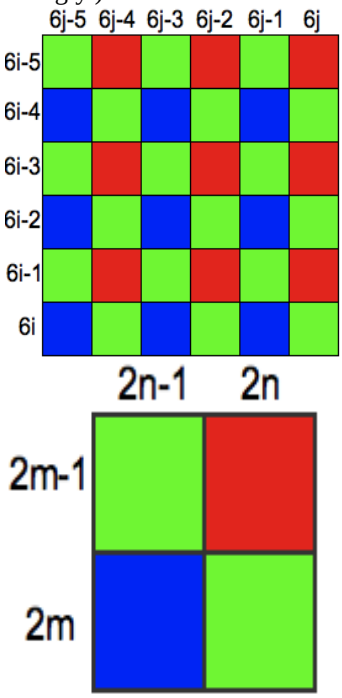

Fig.11. (a) The horizontal and vertical indexes of the (i, j) th 6x6 block in original CFA image (b) The (m,n)th 2 x2 sub-block in the (i,j)th 6x6 block of mosaic image

It is assumed that image is stationary within a small region, i.e., a 2 x2 sub-block in Fig.11 (b), and so adjacent Red, Green and Blue color components can be combined into color vectors [19], which we denote as "pseudo-pixel". Thus a 2x2 sub-block in Fig. 11(b) will have two pseudo-pixels. Since we do not know which pseudo-pixel (if any) corresponds to the actual local color information of the subblock, we can form an unbiased estimate by the average of surrounding pseudo-pixel values. However, merely taking an arithmetic average of the pseudo-pixels is equivalent to bilinear interpolation and may lead to smearing. Instead, to preserve edges, we use the maximum likelihood estimate approach under the constraint that one of the input vectors is chosen to be the output,

$$\begin{aligned} &\underset{\hat{P}}{\text{minimize}} \quad \sum_{k=1}^{K} \|\hat{P} - P_k\|_2 \\ &\text{subject to} \quad \hat{P} \in \{P_k | k = 1, 2, \cdots, K\} \end{aligned} \qquad (1)$$

where $P_k = [p_{k1}, p_{k2}, p_{k3}]^T$ represents a three-component (R,G and B) pseudo-pixel. P is the estimated pseudo-pixel that may best represent the local information of current sub-block. For the (m,m)th sub-block in Fig. 4(b), there are two pseudo-pixels: $P_1(m,n) = [R(2m-1, 2n), G(2m-1, 2n-1), B(2m, 2n-1)]^T$ and $P_2(m,n) = [R(2m-1,2n), G(2m, 2n), B(2m, 2n-1)]^T$. Given only two vectors, the solution of (1) is not unique. As is commonly down with scalar medians, in those cases we use the mean of the two vectors, given by

$$\hat{P}(m,n) = \begin{bmatrix} \hat{R}(m,n) \\ \hat{G}(m,n) \\ \hat{B}(m,n) \end{bmatrix} = \begin{bmatrix} R(2m-1,2n) \\ \frac{G(2m-1,2n-1)+G(2m,2n)}{2} \\ B(2m,2n-1) \end{bmatrix} \qquad (2)$$

Recall that one pixel in S corresponds to one 6 x 6 block (nine sub-blocks) in L_{CFA}, and according to the pattern of subpixel-based decimation we will take three subpixels of a pixel from different subblocks, each from one sub-block. Most of existing subpixel-based down-sampling methods perform horizontal subsampling [5], due to the fact that the red, green, blue subpixels of a typical LCD display are arranged in a horizontal manner. However, as Lu noted in [20], if the edge direction is parallel to the sampling direction, there is little apparent resolution improvement. To achieve improved resolution in all four directions (Horizontal, Vertical, Diagonal, and Anti- Diagonal), we will choose the sampling direction adaptively according to the local edge information.

Traditionally, we can use indirect approach to extract gradient information on mosaic image, i.e., apply existing demosaicing methods and convert the demosaiced full color image to the luminance map, then a Sobel-based edge detector is applied on the luminance map [21] [14]. However, such approach may lead to inaccurate estimation of gradient and high computational complexity. To extract more accurate edge information, we will directly embed Sobel operator into Bayer image. Recall that the estimated pseudo-pixel of the (m, n) th sub-block is given in (2), and hence the estimated luminance value may be approximated by (3). Given the estimated luminance map, the gradient response of the (i, j) th block in horizontal direction is given in (4).

$$\begin{aligned} \hat{Y}(m,n) &= \tfrac{3}{10}\hat{R}(m,n) + \tfrac{1}{10}\hat{B}(m,n) + \tfrac{6}{10}\hat{G}(m,n) \\ &= \tfrac{3}{10}R(2m-1,2n) + \tfrac{1}{10}B(2m,2n-1) \\ &+ \tfrac{3}{10}(G(2m-1,2n-1) + G(2m,2n)) \end{aligned} \qquad (3)$$

$$\begin{aligned} \Delta Y^{H}_{CFA}(i,j) = &(\hat{Y}(3i-2,3j) + 2\hat{Y}(3i-1,3j) + \hat{Y}(3i,3j)) \\ &-(\hat{Y}(3i-2,3j-2) + 2\hat{Y}(3i-1,3j-2) + \hat{Y}(3i,3j-2)) \end{aligned} \qquad (4)$$

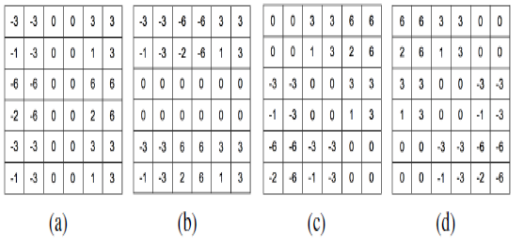

Fig. 12. SL-based mask in four directions: (a) horizontal mask (b) vertical mask (c) diagonal mask (d) anti-diagonal mask.

Combining (3) and (4), we have $\Delta Y^{H}_{CFA}(i,j)$ in (5), which is directly applied on Bayer image. Similarly, we can obtain $\Delta Y^{V}_{CFA}(i,j)$, $\Delta Y^{D}_{CFA}(i,j)$, $\Delta Y^{AD}_{CFA}(i,j)$. For avoiding the floating point computation, the coefficients in the masks are normalized into integers in advance and the four normalized

Sobel- Luminance-based masks are shown in Fig.12. These four masks are directly applied on CFA image, which can effectively determine the local edge direction for any (i, j) [th] block, denoted as Dir(i,j). We further denote the direction of subpixel-based decimation in (i,j)[th] block as Dir↓(i; j), which is adaptively chosen to be the perpendicular direction of Dir(i,j),

$$\mathrm{Dir}_{\downarrow}(i,j)=\begin{cases} \mathrm{H}, & \text{if } \mathrm{Dir}(i,j)=V \\ \mathrm{V}, & \text{if } \mathrm{Dir}(i,j)=H \\ \mathrm{D}, & \text{if } \mathrm{Dir}(i,j)=AD \\ \mathrm{AD}, & \text{if } \mathrm{Dir}(i,j)=D \end{cases}$$

One of the four cases in (6) is demonstrated in Fig. 13, where the local edge direction (Dir(i, j)) is anti-diagonal direction, and the direction for subpixel-based decimation (Dir↓ (i; j)) is diagonal direction. In other words, we will copy the red, green, blue components of the (i, j)th pixel in S from three different sub-blocks of (i, j)[th] block in L_{CFA} along diagonal

$$r_{i,j}=\hat{R}_{3i-2,3j-2}, g_{i,j}=\hat{G}_{3i-1,3j-1}, b_{i,j}=\hat{B}_{3i,3j}$$

direction

Unfortunately, direct application of subpixel-based decimation may cause local color unbalance, introducing severe color fringing artifacts. Several algorithms have been proposed to suppress color distortion. However, to the best of our knowledge, most of existing methods work merely in horizontal direction [6] [7] [8]. In [20], an optimal 2-D minimum mean square error subpixel-based downsampling scheme is proposed and the corresponding solution can be implemented by a 2-D linear filter followed by subpixel-based downsampling. Such 2-D linear prefilter is effective in suppressing color fringing artifacts and can be well implemented in our adaptive directional subpixel-based decimation. Therefore, as shown in Fig. 14, the proposed AJDSD is implemented by firstly extracting pseudopixels from the corresponding sub-blocks based on the maximum likelihood estimation, then the extracted pseudo-pixels are filtered by the 2-D optimal linear filter, followed by adaptive subpixel-based down-sampling processing.

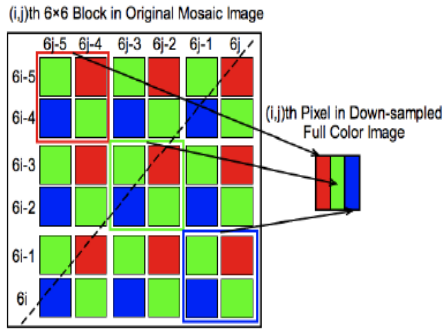

Fig. 13. Pattern of AJDSD

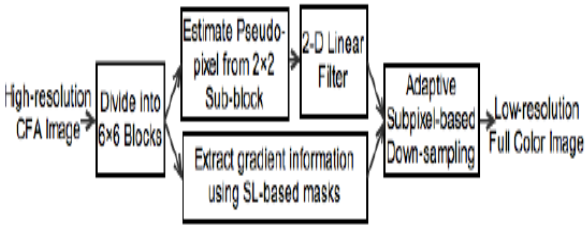

Fig. 14. Diagram of adaptive joint demosaicing and subpixel-based down-sampling scheme.

VI. FAST FREQUENCY DOMAIN ANALYSIS APPROACH FOR JOINT DEMOSAICING AND SUBPIXEL BASED DOWNSAMPLING

In this, sub pixel-based techniques are explored to the problem of joint demosaicing and down-sampling. As one pixel in the stripe LCD contains three sub pixels, there exists natural down-sampling pattern for 3:1 down-sampling, while the Bayer color filter array (CFA) pattern repeats itself for every 2 x 2 block. For every pixel within the 2x 2 block, only one color is sampled. We observe that 3:1 sub pixel-based down-sampling cannot be applied to the Bayer sampled image directly because the Bayer CFA pattern does not repeat for 3x 3 blocks and the required color for sub pixel-based down-sampling is very often missing. While any one pixel of the Bayer CFA pattern does not have all three color components available, a 2x 2 block (which we will call a "super-pixel") will always have some available red, green, and blue components (one red, one blue, and two green, to be exact). Thus, we can apply 3:1 sub pixel- based down-sampling to the super-pixels. As a result, we are effectively doing a 6:1 down-sampling on the original Bayer sampled image. So there is a large image of size 6M X 6N and a down-sampled version (small image) of size M X N.

In this section, i use the term "large" and the symbol L (which stands for "large") to refer to an image of size 6M X 6N. Also i use the term "small" and the symbol S (which stands for "small") to refer to an image of size M X N. For example, we use L to represent original high resolution input full color image of size 6M X 6N, and we use L_{CFA} to represent the Bayer image obtained by applying Bayer CFA to L. Note that the unavailable color components in are represented as zero. Also we use simply S to represent the down-sampled low resolution full-color image of size M X N. Without loss of generality, the RGB color components of L_{CFA} can be represented by those in L as,

$$R_{\mathrm{CFA}}(i,j)=\begin{cases} R(i,j), & \text{for } i=2k-1, j=2l, \\ 0, & \text{otherwise;} \end{cases}$$

$$B_{\mathrm{CFA}}(i,j)=\begin{cases} B(i,j), & \text{for } i=2k, j=2l-1, \\ 0, & \text{otherwise;} \end{cases}$$

$$G_{\mathrm{CFA}}(i,j)=\begin{cases} G(i,j), & \text{for } \{i=2k-1, j=2l-1\}, \\ & \text{or } \{i=2k, j=2l\}, \\ 0, & \text{otherwise} \end{cases}$$

where k=1,…..3M, l=1,…….3N and i=1,…….6M,j=1,…….6N.

a) Frequency Analysis Of Bayer Image

Given the spatial multiplexing of RGB components of any image X (such as $L_{CFA)}$, we define an auxiliary luminance image I_X , where I_X(i,j)is the average of the three corresponding color components of X [i.e.,R_X(i,j),G_X(i,j) B_X(i,j)], which reflects the luminance of X in a simple way. The luminance of L_{CFA};

$$I_{CFA}(i,j)=\frac{1}{3}\left(R_{CFA}(i,j)+G_{CFA}(i,j)+B_{CFA}(i,j)\right)$$
$$=\frac{1}{3}\left(R(i,j)\Delta^{R}_{CFA}+G(i,j)\Delta^{G}_{CFA}+B(i,j)\Delta^{B}_{CFA}\right)$$
$$=\frac{1}{3}\sum_{C}C(i,j)\Delta^{C}_{CFA}(i,j)$$

where C stands for R, G or B and $\Delta^{C}_{CFA}(i,j)$ is the corresponding RGB modulation function. According to the convolution theorem, the Fourier transform of I_{CFA} can be computed as

$$\hat{I}_{CFA}(u,v)=\frac{1}{3}\sum_{p}\hat{C}^{p}(u,v)*\hat{\Delta}^{p}_{CFA}(u,v)$$

where ˆ represents the discrete time Fourier transform with zero padding outside the support of I_{CFA} and Δ^{C}_{CFA}, and * is the convolution operator.

$$\hat{I}_{CFA}(u,v)=\frac{1}{3}\cdot 1_3^{T}\begin{bmatrix}\hat{C}_2\left(u+\frac{1}{2},v+\frac{1}{2}\right) & \hat{C}_1\left(u+\frac{1}{2},v\right) & \hat{C}_2\left(u+\frac{1}{2},v-\frac{1}{2}\right)\\ -\hat{C}_1\left(u,v+\frac{1}{2}\right) & \hat{Y}(u,v) & -\hat{C}_1\left(u,v-\frac{1}{2}\right)\\ \hat{C}_2\left(u-\frac{1}{2},v+\frac{1}{2}\right) & \hat{C}_1\left(u-\frac{1}{2},v\right) & \hat{C}_2\left(u-\frac{1}{2},v-\frac{1}{2}\right)\end{bmatrix}1_3$$

where $1_3=[1\ 1\ 1]^T$ and

$$\begin{cases}\hat{Y}(u,v)=\frac{1}{4}\hat{R}(u,v)+\frac{1}{2}\hat{G}(u,v)+\frac{1}{4}\hat{B}(u,v)\\ \hat{C}_1(u,v')=\frac{1}{4}\hat{R}(u,v)-\frac{1}{4}\hat{B}(u,v)\\ \hat{C}_2(u,v)=-\frac{1}{4}\hat{R}(u,v)+\frac{1}{2}\hat{G}(u,v)-\frac{1}{4}\hat{B}(u,v).\end{cases}$$

In Fig. 15, we evaluate the magnitudes of $\hat{Y}$, $\hat{C1}$ and respectively. We can see that although all three spectra $\hat{Y}$, and are weighted sums of , $\hat{G}$ a ,their magnitudes can be very different. Both $\hat{C1}$ and appear to be more compact than .This phenomenon can be interpreted as follows. Each color component such as R can be decomposed into a low-frequency term R_l and a high frequency term R_h, and since the high frequency components of different colors tend to be similar [11,i.e., we have $_h(u,v)$ ≈ $_h(u,v)$ ≈ $_h(u,v)$,we have

$$\hat{C}_1(u,v)=\frac{1}{4}\hat{R}(u,v)-\frac{1}{4}\hat{B}(u,v)$$
$$=\frac{1}{4}(\hat{R}_l+\hat{R}_h)-\frac{1}{4}(\hat{B}_l+\hat{B}_h)]$$
$$\approx\frac{1}{4}(\hat{R}_l-\hat{B}_l).$$

Therefore, is mainly composed by a low frequency signal. Similar argument can be applied to . Different from and whose energy is mainly in low frequency, contains significant high frequency energy since

$$\hat{Y}(u,v)=\frac{1}{4}\hat{R}(u,v)+\frac{1}{2}\hat{G}(u,v)+\frac{1}{4}\hat{B}(u,v)$$
$$\approx\left(\frac{1}{4}\hat{R}_l+\frac{1}{2}\hat{G}_l+\frac{1}{4}\hat{B}_l\right)+\hat{G}_h.$$

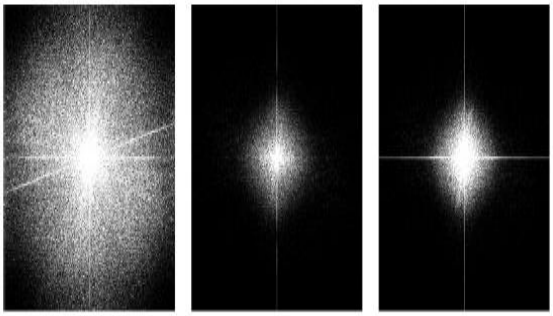

Fig.15. (a) Magnitude of $\hat{Y}$. (b) Magnitude of $\hat{C1}$. (c) Magnitude of $\hat{C2}$.

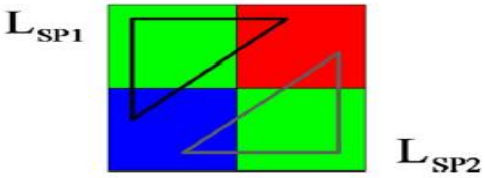

Fig.16. Two super-pixels inside a 2x2 block of L_{CFA} .

b) Frequency Analysis Of Subpixel-Based Down-Sampled Image

Recall that any one pixel of L_{CFA} does not have all three color components available, a 2 X 2 block of L_{CFA} (which we will call a "super-pixel") will always have some available red, green, and blue components. With this, we define two 3M X 3N super-pixel images L_{SP1} and L_{SP2} in Fig. 16, where the RGB color components of the super-pixel images are;

$$R_{SP_1}(k,l)=R_{SP_2}(k,l)=R(2k-1,2l),$$
$$B_{SP_1}(k,l)=B_{SP_2}(k,l)=B(2k,2l-1),$$
$$G_{SP_1}(k,l)=G(2k-1,2l-1),$$
$$G_{SP_2}(k,l)=G(2k,2l)$$

where k=1,……,3M,L=1,……,3N . Given super-pixel images L_{SP1} and L_{SP2}, subpixel-based down-sampling can be directly applied to obtain low resolution full color image.

As discussed in [12], subpixel-based down-sampling can be done in horizontal, diagonal, or anti-diagonal directions. (It does not make sense to sample in vertical direction as RGB subpixels are arranged in horizontal way.)

In Fig. 17 (a), an experiment is done by down-sampling an artificial large image with regular line width using direct pixel-based down-sampling (DPD), direct subpixel-based down-sampling (DSD), and diagonal direct subpixel-based down-sampling (DDSD) methods.

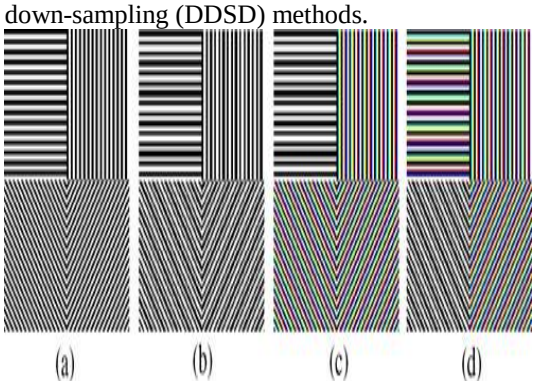

Fig.17. (a) Original L image. (b) Result of DPD. (c) Result of DSD.(d)Result of DDSD

DSD and DDSD are very similar except that DSD subsamples in the horizontal direction while DDSD subsamples in the diagonal direction. The straight-forward DPD gives an image with irregular line spacing, which is bad. Both DSD and DDSD preserve the line regularity for lines in 3 directions at the price of color fringing artifacts. They have no effect on the 4th direction (horizontal for DSD and diagonal for DDSD). Horizontal lines occur more often than diagonal lines in general and thus can conclude that DDSD may be more useful than DSD in general. A similar experiment was done also for anti-diagonal down-sampling.Thus noted that [12] diagonal and anti-diagonal are essentially the same. In [13], further studied the frequency characteristics of DPD, DSD, and DDSD.So can conclude that the spectral overlap (aliasing) in DDSD is considerably less than that in DSD, and thus DDSD is more effective in retaining high frequency details than DSD. Therefore, chose to use DDSD instead of DSD. Fig.18 depicts the case we apply DDSD on two super-pixel images, where the RGB color components of the DDSD image are

$$\begin{cases} R_{DDSD}(i,j)=\begin{cases} R_{SP}(i,j), & \text{for } (i=3m-2, j=3n-2), \\ 0, & \text{otherwise;} \end{cases} \\ G_{DDSD}(i,j)=\begin{cases} G_{SP}(i,j), & \text{for}(i=3m-1, j=3n-1), \\ 0, & \text{otherwise;} \end{cases} \\ B_{DDSD}(i,j)=\begin{cases} B_{SP}(i,j), & \text{for } (i=3m, j=3n), \\ 0, & \text{otherwise} \end{cases} \end{cases}$$

where , m=1,2,….,M, n=1,2,…..,N.

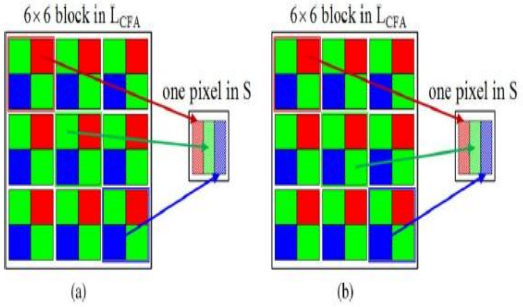

Fig.18. Two patterns of diagonal direct subpixel-based down-sampling (DDSD) on L_{CFA}. (a)L_{DDSD1} (b) L_{DDSD2}

Note that due to the two different green components in one super-pixel (or 2 X 2 block of L_{CFA}), the green component of DDSD image ($G_{DDSD}(i,j)$) is given by $G_{CFA}(i,j)$ for (i=6m-3,j=6n-3) or (i=6m,j=6n-1),as shown in Fig.18.
Similar to (2), we define

$$I_{DDSD}(i,j)=\frac{1}{3}\left(R_{DDSD}+G_{DDSD}+B_{DDSD}\right)$$

The frequency response of I_{DDSD} can be obtained by computing the Fourier transform of (9).There will exist two cases of $\hat{I}_{DDSD}$ due to the two sampling patterns of Δ^{G}_{DDSD} in L_{DDSD}, which we denote as $\hat{I}_{DDSD1}$ and $\hat{I}_{DDSD2}$, respectively.

$$\hat{I}^{3\times3}_{DDSD_1}=1^{T}_{3}\begin{bmatrix} \hat{C}_{B_1}(u^{+},v^{+}) & \hat{C}_{R_1}(u^{+},v) & \hat{Y}_1(u^{+},v^{-}) \\ \hat{C}_{01}(u,v^{+}) & \hat{Y}_0(u,v) & \hat{C}_{02}(u,v^{-}) \\ \hat{Y}_2(u^{-},v^{+}) & \hat{C}_{R_2}(u^{-},v) & \hat{C}_{B_2}(u^{-},v^{-}) \end{bmatrix}1_3$$

where $u^{\pm}=u\pm(1/6), v^{\pm}=u\pm(1/6)$. $\hat{Y}_0$, $\hat{Y}_1$, and $\hat{Y}_2$ are

$$\begin{cases} \hat{Y}_0(u,v)=\frac{1}{3}\left(\hat{R}(u,v)+\hat{G}(u,v)+\hat{B}(u,v)\right) \\ \hat{Y}_1(u,v)=\frac{1}{12}\left(a\hat{R}(u,v)+\hat{G}(u,v)+a\hat{B}(u,v)\right) \\ \hat{Y}_2(u,v)=\frac{1}{12}\left(-b\hat{R}(u,v)+\hat{G}(u,v)-b\hat{B}(u,v)\right) \end{cases}$$

where $a=e^{j(\pi/3)}$ and $b=e^{j(2\pi/3)}$. $\hat{C}_{01}, \hat{C}_{02}, \hat{C}_{R_1}, \hat{C}_{R_2}, \hat{C}_{B_1}$, and $\hat{C}_{B_2}$ are

$$\begin{cases} \hat{C}_{01}(u,v)=\frac{1}{6}\left(a\hat{R}(u,v)-\hat{G}(u,v)-b\hat{B}(u,v)\right) \\ \hat{C}_{02}(u,v)=\frac{1}{6}\left(-b\hat{R}(u,v)-\hat{G}(u,v)+a\hat{B}(u,v)\right) \\ \hat{C}_{R_1}(u,v)=\frac{1}{12}\left(b\hat{R}(u,v)-\hat{G}(u,v)+\hat{B}(u,v)\right) \\ \hat{C}_{R_2}(u,v)=\frac{1}{12}\left(-a\hat{R}(u,v)-\hat{G}(u,v)+\hat{B}(u,v)\right) \\ \hat{C}_{B_1}(u,v)=\frac{1}{12}\left(-\hat{R}(u,v)+\hat{G}(u,v)-b\hat{B}(u,v)\right) \\ \hat{C}_{B_2}(u,v)=\frac{1}{12}\left(-\hat{R}(u,v)+\hat{G}(u,v)+a\hat{B}(u,v)\right) \end{cases}$$

Similarly,

$$\hat{I}^{3\times3}_{DDSD_2}=1^{T}_{3}\begin{bmatrix} -b\hat{C}_{R_2}(u^{+},v^{+}) & a\hat{C}_{01}(u^{+},v) & \hat{Y}_1(u^{+},v^{-}) \\ -a\hat{C}_{B_2}(u,v^{+}) & \hat{Y}_0(u,v) & b\hat{C}_{B_1}(u,v^{-}) \\ \hat{Y}_2(u^{-},v^{+}) & -b\hat{C}_{02}(u^{-},v) & a\hat{C}_{R_1}(u^{-},v^{-}) \end{bmatrix}1_3.$$

In Fig. 19, we show the magnitudes of $\hat{I}_{DDSD1}$ and $\hat{I}_{DDSD2}$. For both of them, we can clearly see nine replicated spectra situated at the locations of the Dirac functions (u,v), where u € {-(1/6),0,1/6} and v € {-(1/6),0,1/6}. As we

expected, the three "luminance" spectra ($\hat{Y}_1$, $\hat{Y}_0$ and $\hat{Y}_2$) are located in the anti-diagonal direction in both $\hat{I}_{DDSD1}$ and $\hat{I}_{DDSD2}$ due to the diagonal sampling direction of DDSD. While $\hat{C}_0$, $\hat{C}_R$ and $\hat{C}_B$ are located differently in $\hat{I}_{DDSD1}$ and $\hat{I}_{DDSD2}$, due to the different sampling locations of the G component in $\hat{L}_{DDSD1}$ and $\hat{L}_{DDSD2}$.

To examine the difference between $\hat{Y}$ and $\hat{C}_0$, $\hat{C}_R$ and $\hat{C}_B$ we further show their magnitudes in Fig.20. $\hat{Y}_1$, $\hat{Y}_0$ and $\hat{Y}_2$ contain significant high frequency energy, while $\hat{C}_{01}$, and $\hat{C}_{02}$ are mainly low frequency signals. For $\hat{C}_R$ and $\hat{C}_B$, the high frequency energy of $\hat{C}_R$ and $\hat{C}_B$ is mainly determined by the high frequency of R and B components, respectively. In other words, the magnitudes of $\hat{C}_R$ and $\hat{C}_B$ may vary a lot with different source images.

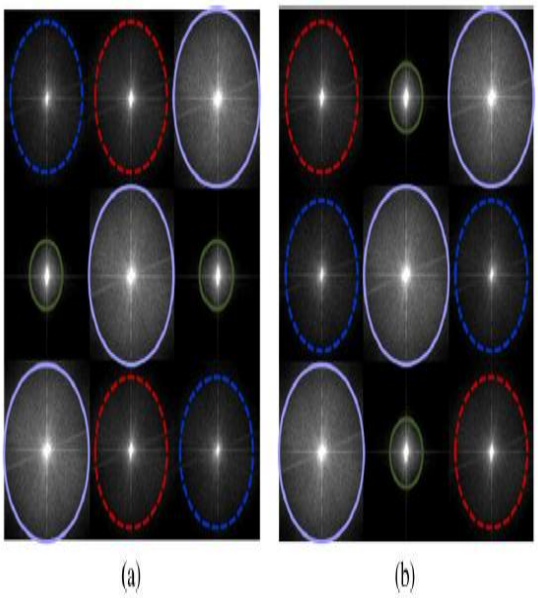

Fig. 19. Magnitudes of $\hat{I}_{DDSD1}$ and $\hat{I}_{DDSD2}$. (a) $\hat{I}_{DDSD1}$. (b) $\hat{I}_{DDSD2}$

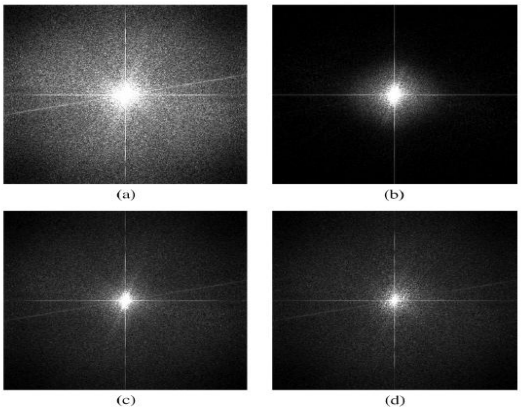

Fig.20. Magnitudes of (a)$\hat{Y}1$(b) $\hat{C}_{01}$ (c) $\hat{C}_{R1}$.(d) $\hat{C}_{B1}$.

c) Cut-Off Frequency Selection

With the low-frequency nature of $\hat{C}_{01}$, and $\hat{C}_{02}$, the center spectrum $\hat{Y}_0$ in $\hat{I}_{DDSD1}$ or $\hat{I}_{DDSD2}$ has relatively low overlapping with horizontal and vertical neighboring spectra, even though its overlapping with anti-diagonal neighboring spectra can be considerable. To suppress aliasing, we need to remove the aliasing effect of all other 8 neighboring replicated spectra on the center spectrum.

According to Nyquist criterion, a signal bandlimited to W must be sampled at $f_s \geq 2W$ [14]. Suppose an image X is obtained by sampling (critically) at such a sampling frequency f_s = 2W.If X is to be k: 1 downsampled,the effectively sampling frequency will be reduced to $f_s' = f_s/k$. One way to prevent aliasing is to apply a low-pass (anti-aliasing) filter to the signal with a cutoff frequency of $f_s'/2 = f_s/2k$. For the image X , recall that the digital frequency of 1 corresponds to analog frequency of f_s . Thus the digital cutoff frequency of the low-pass filter is 1/2k. For us, k=6. Thus the digital cutoff frequency is 1/12.

Nevertheless,with the smaller amount of overlap between $\hat{Y}_0$ and $\hat{C}_0$, $\hat{Y}_0$ and $\hat{C}_R$, $\hat{Y}_0$ and $\hat{C}_B$, it is possible for us to use a higher cut-off frequency to preserve more signal detail in $\hat{Y}_0$.

VII. COMPARISON

In experiments, FFA-JDSD and AJDSD are compared against two "Demosaicing first and Down-sampling-later" methods. The original true color image L of size 6M X 6N is first down-sampled to a Bayer CFA image L_{CFA} of size 6M X 6N. From L_{CFA}, the full color image S of size M X N is to be reconstructed using two "Demosaicing- first and Down-sampling later" methods.The two demosaicing algorithms are Bilinear Interpolation (BI) and Edge weighted Interpolation (EDGE).

a) AJDSD

i)SPEED IMPROVEMENT

To measure the computational complexity of AJDSD and three "demosaicing-first and downsampling-later" methods (BI and EDGE), in Table 1 we depict the CPU running time when processing 712 X 512 full color images. It is obvious that AJDSD performs favorably compared to BI, and EDGE. Generally speaking, the CPU time consuming of AJDSD is about 60% of the EDGE. This is mainly because BI and EDGE are "demosaicing-first and downsampling-later" methods, and the demosaicing method EDGE is of high computational complexity, while AJDSD does not need to demosaic each and every pixel.

Table 1.
CPU time (seconds) of BI/EDGE and AJDSD.

IMAGE	BI	EDGE	AJDSD
1	0.45	0.53	0.37
2	0.33	0.54	0.39
3	0.40	0.54	0.36
4	0.39	0.53	0.37
5	0.32	0.53	0.36
Avg	0.37	0.54	0.37

ii) VISUAL QUALITY

I used a sharpness measure which computes the average of Directional High frequency Energy (DHE):

$$\mathrm{DHE}(X) = \frac{\frac{1}{4}\sum_{k=1}^{4} \|H^k * X\|_1}{\frac{1}{4}\sum_{k=1}^{4} \|H^k * \mathrm{PDAF}\|_1}$$

For any image X to be measured, we compute the average of directional high-frequency energy by convolving a 1-D high pass filter in four directions. Basically, the four filters are simply the same 1-D high pass filter H^k = [1 - 1] applied in the horizontal (k=1), vertical (k=2), diagonal (k=3) and anti-diagonal (k=4) directions. The reference images are computed by applying Pixel-based Down-sampling with Anti-aliasing Filter (PDAF) to the original true color (non Bayer-filtered) images. By definition, the values of DHE are positive numbers. A higher value indicates that there is more luminance high frequency energy which suggests higher apparent luminance resolution. Observed that the DHE values of AJDSD are larger than 1, which suggests that AJDSD provides clearer and sharper down-sampled images than PDAF.

As expected, the improvements are especially obvious in edge regions, i.e., the window and roof in Fig. 21(b).Some reviewers may find that there exists somewhat color fringing artifacts in AJDSD. However, it is less objectionable.

Table 2.

Sharpness Measure: Directional High-frequency Energy

IMAGE	BI	EDGE	AJDSD
1	0.965	0.991	1.332
2	0.979	0.996	1.364
3	0.981	0.998	1.254
4	0.975	1.002	1.266
5	0.981	1.006	1.323
Avg	0.976	0.994	1.289

(a)

(b)

Fig21. Downsampled images for test image
(a) BI (b) AJDSD

b) FFA-JDSD

i) COMPUTATIONAL COMPLEXITY

Computed the amount of operations (i.e., multiplication, addition, and compare) of various methods, as shown in Table 3. For FFA-JDSD, we need to apply 2-D FFT to I_{CFA} (of size M X N). It is clear that the operation of multiplications of the 2-D FFT is basically MN $\log_2$MN. Due to symmetry, the operation of multiplications is basically 6 per down-sampled pixel location. Therefore, the total operation of multiplications is basically MN $\log_2$MN +6MN/k^2 for FFT-JDSD, where k is the down-sampling ratio. As shown in Table 3, the computation and implementation complexities of FFA-JDSD are slightly higher than that of BI, while is considerably (if not significantly) lower than EDGE. This is mainly because FFA-JDSD does not require demosaicing each and every pixel.

Table 3

Computational complexity

	"Demosaicking-first and Down-sampling-later" Methods		Proposed
	BI	EDGE	FFA-JDSD
adds	$15MN+\frac{15}{k^2}MN$	$59MN+\frac{15}{k^2}MN$	$18MN+\frac{20}{k^2}MN$
multiplies	$5MN+\frac{16}{k^2}MN$	$17MN+\frac{16}{k^2}MN$	$18MN+\frac{6}{k^2}MN$

ii) VISUAL QUALITY

I used High frequency Energy (HFE) to measure the luminance sharpness of image X.

$$\mathrm{HFE}(X)=\frac{\frac{1}{4}\sum_{k=1}^{4}\left|H^k * X\right|_1}{\frac{1}{4}\sum_{k=1}^{4}\left|H^k * PDAF\right|_1}.$$

By definition, HFE is non-negative. A larger HFE indicates that there is more luminance high frequency energy, which suggests higher apparent luminance sharpness. Table 4 depicts the HFE values of concerned methods. As we expected, BI produces the smallest value of HFE due to the blurring artifacts caused by simple bilinear demosaicing. The HFE values of EDGE are close to 1, suggesting it can achieve comparable sharpness as the reference image PDAF. While the HFE value of FFA-JDSD is considerably (if not significantly) larger than other methods including the reference image PDAF, suggesting that FFA-JDSD retains more high frequency detail than BI and EDGE, leading to the sharpest down-sampled images. Experimental results of "light house" using concerned methods (BI, EDGE, and FFA-JDSD) are shown in Fig.22. FFA-JDSD (with highest HFE value) can achieve the sharpest down-sampled result compared to other "Demosaicing-first and Down-sampling-later" methods, especially in regions labeled with red circles. For regions with superior high frequency details, i.e., the fence in "light house", color artifacts are obvious in poorly designed demosaicing method (i.e., BI), but less noticeable in EDGE, and FFA-JDSD.

Table 4

Luminance sharpness measure(HFE)

High frequency energy			
Image	BI	EDGE	FFA-JDSD
1	0.988	0.997	1.426
2	0.994	0.999	1.258
3	0.991	1.001	1.305
4	0.984	1.002	1.442
5	0.988	1.002	1.387
6	0.987	1.002	1.471
7	0.984	1.000	1.336
8	0.990	0.999	1.370
9	0.986	1.000	1.374
ave	0.988	1.000	1.374

(a) (b)

Fig.22. Experimental results using "Demosaicing-first and Down-sampling-later" methods and FFA-JDSD

Although AJDSD and FFA-JDSD may cause color fringing artifacts occasionally, it is less objectionable. This is mainly because our human eyes are much more sensitive to the high frequency of luminance than to that of chrominance.

Merits of AJDSD over FFAJDSD includes: the sampling direction adaptively according to the local edge information and 2-D linear prefilter is effective in suppressing color fringing artifacts. But considering visual quality FFAJDSD is better.

VIII. Conclusion

To show single-sensor camera images on a lower resolution display, two steps are needed: demosaicing and down-sampling. Unfortunately, the color artifacts introduced in demosaicing may be magnified in subsequent down-sampling process and vice versa. This paper presented a joint demosaicing and subpixel-based downsampling scheme for Bayer images, where subpixel-based decimation is applied i)adaptively and ii)FFA, directly in Bayer domain itself. The frequency characteristics of FFAJDSD is further investigated, based on which, the cut-off frequency of the low-pass filter for JDSD can be effectively extended beyond the Nyquist frequency. Simulation results show that the proposed algorithms are superior to conventional methods, in terms of highly reducing computational complexity and preserving more high frequency details,thus achieves much sharper and clearer results.

References

[1] B. E. Bayer, "Color imaging array," U.S. Patent 3 971 065, Jul. 1976.
[2] R. Lukac and K. N. Plataniotis, "Color filter arrays: Design and performance analysis," *IEEE Trans. Consum. Electron.*, vol. 51, no. 4, 2005.
[3] P. Longere, X. Zhang, P. B. Delahunt, and D. H. Brainard, "Perceptual assessment of demosaicing algorithm performance," *Proc. IEEE*, Jan. 2002.
[4] R. Lukac, K. N. Plataniotis, and D. Hatzinakos, "Color image zooming on the Bayer pattern," *IEEE Trans. Circuits Syst. Video Technol.*, vol. 15, no. 11, pp. 1475–1492, Nov. 2005.
[5] S. Gibson, Sub-Pixel Font Rendering Technology.
[6] C. Betrisey *et al.*, "Displaced filtering for patterned displays," in *SID Int. Symp. Digest of Technical Papers*, 2000, vol. 31, pp. 296–301.
[7] S. Daly, "Analysis of subtriad addressing algorithms by visual system models," in *SID Int. Symp. Digest of Technical Papers*, 2001, vol. 32.
[8] M. A. Klompenhouwer, G. Haan, and R. A. Beuker, "Subpixel image scaling for color matrix displays," *J. Soc. Inf. Display*, vol. 11, 2003.
[9] L. Fang and O. C. Au, "Subpixel-based image down-sampling with min-max directional error for stripe display," *IEEE J. Select. Topics Signal Process.*, vol. 5, no. 2, pp. 240–251, Apr. 2011.
[10] P. S. R. Diniz, *Digital Signal Processing*. Cambridge, U.K.: Cambridge Univ. Press, 2010.
[11] N. X. Lian, L. Chang, Y. P. and V. Zagorodnov, "Adaptive filtering for color filter array demosaicking," *IEEE Trans. Image Process.*,Oct. 2007.
[12] L. Fang, O. C. Au,K. Tang and H.Wang, "Novel 2-DMMSE subpixel based image down-sampling," *IEEE Trans. Circuits Syst. Video Technol.*
[13] L. Fang, O. C. Au, K. Tang, and A. K. Katsaggelos, "Anti-aliasing filter design for subpixel down-sampling via frequency domain analysis," *IEEE Trans. Image Process.*, to be published.
[14] R. C. Gonzalez and E. Richard, "Woods, digital image processing," *Publishing House Electron. Ind.*, pp. 420–450, 2005.
[15] E. Y. Lam and J. W. Goodman, "A mathematical analysis of the DCT coefficient distributions for images," *IEEE Trans. Image Process.*,Oct. 2000.
[16] T. Sakamoto, C. Nakanishi, and T. Hase, "Software pixel interpolation for digital still camera suitable for a 32-bit MCU," *IEEE Trans. Consum. Electron.*, vol. 44, no. 4, pp. 1342–1352, Nov. 1998.
[17] K. Hirakawa and T.W. Parks, "Adaptive homogeneity-directed demosaicing algorithm," *IEEE Trans. Image Process.*, vol. 14, Mar. 2005.
[18] L. Zhang and X. Wu, "Color demosaicking via directional linear minimummean square-error estimation," *IEEE Trans. Image Process.*,2005.
[19] R. Lukac, K.N. Plataniotis, and D. Hatzinakos, "Color image zooming on the Bayer pattern," Circuits and Systems for Video Technology, IEEE Transactions on, vol. 15, no. 11, pp. 1475–1492, 2005.
[20]L. Fang and O.C. Au, "Novel 2-D MMSE subpixel-based image down-sampling for matrix
displays," in Acoustics Speech and Signal Processing (ICASSP), 2010 IEEE International Conference on. IEEE, 2010.
[21] K.L. Chung, W.J. Yang, W.M. Yan, and C.C. Wang, "Demosaicing of color filter array captured
images using gradient edge detection masks and adaptive heterogeneity-projection," Image Processing, IEEE Transactions on, vol. 17, no. 12, pp. 2356–2367, 2008.

Lekshmi P R received Btech in Electronics and Communication Engg from CUSAT University Kerala.Currently pursing Mtech in Signal Processing at Govt Engg college, Cherthala under Cochin University Of Science And Technology. Areas of interest includes Signal Processing, Image Processing, Artificial Neural Networks.